



## EFFECTIVE STRESS INTENSITY FACTOR FOR CRACK OF INTERGRANULAR MORPHOLOGY

J. HORNÍKOVÁ<sup>1)</sup>, P. ŠANDERA<sup>2)</sup> AND J. POKLUDA<sup>2)</sup>

<sup>1)</sup>*Institute of Mechanics of Solids*, <sup>2)</sup>*Institute of Physical Engineering*,  
*Brno University of Technology, Faculty of Mechanical Engineering, Technická 2,*  
*61669 Brno, Czech Republic*

### ABSTRACT

The microtortuosity of the crack front induces a local mixed mode 1+2+3 even in case of the remote mode I loading. It causes a shielding effect not taken into account in standard procedures for evaluation of fracture characteristics. The main aim of this work is to perform a 3D BEM analysis of the elastic stress-strain field at the front of real-like intergranular cracks. Results of this analysis are evaluated in terms of the integral effective stress intensity factor  $k_{eff}$  related to the intergranular crack front. Quantitative estimation of the corresponding shielding level can be used for correcting values of fracture toughness in order to get intrinsic component characterising well the real resistance of grain boundaries against the unstable crack growth initiation.

### KEYWORDS

Effective stress intensity factor, intergranular crack front, shielding effect, ultra high strength steels, boundary element method, CT specimen.

### INTRODUCTION

According to a generally accepted idea [1], the fracture toughness consists of two basic components called *extrinsic* and *intrinsic*. The intrinsic component is associated with the inherent resistance of a material against crack propagation given by the strength of interatomic bonds and matrix plasticity. The extrinsic component is related to the processes reducing the crack driving force as, e.g., the tortuous geometry of the crack (crack branching) or bridging of fracture surfaces.

The technology of enhancing the fracture toughness by means of artificially induced crack branching was successfully used in case of advanced ceramics [2], where the extrinsic component is very significant. This treatment does not seem to be efficient in case of metals due to their more extensive plasticity. A general analysis of the problem of extrinsic component in metallic materials was presented elsewhere [3] and it is beyond the framework of this paper. However, in case of fracture by pure intergranular decohesion typical for environment and low temperatures, the physical meaning of extrinsic component is quite simple. Consequently, this component can be determined exclusively on the basis of 3D models of crack front geometry and principles of linear elastic fracture mechanics.

The aim of this article is to present a method of calculation of the extrinsic component in case of intergranular fracture. Moreover, a simple analytical approximation is discussed enabling to avoid both the cumbersome numerical procedure and the quantitative metallographical analysis. The respective remote mode I, plain strain and small scale yielding case will be assumed further within the framework of the one-parameter LEFM.

### SHIELDING EFFECT AT THE FRONT OF A REAL-LIKE MODEL OF THE INTERGRANULAR CRACK

Due to the tortuous microgeometry, a local mixed mode loading 1+2+3 exists at the intergranular crack front. Considering the external (remote) mode I loading, the friction forces caused by shear modes 2 and 3 are minimised and the crack propagates in a self-similar manner. From the microscopic point of view, the same statistical distribution of local mixed modes along the crack front is repeating in each moment. From the macroscopic point of view, the crack propagates perpendicularly to the external loading direction. Thus, the energetic criterion in terms of local  $k$ -factors can be used for the assessment of the crack stability:

$$k_c = \sqrt{k_I^2 + k_{II}^2 + \frac{4}{\kappa + 1} k_{III}^2}, \quad (1)$$

where  $\kappa = 3 - 4\nu$  for plain strain,  $\kappa = (3 - \nu)/(1 + \nu)$  for plain stress and  $\nu$  is the Poisson ratio. The right hand side represents the local effective stress intensity factor  $k_{eff}$  (normalised to the remote  $K_I$ -value) and the left hand side equals to its normalised local critical value. It is well-known that the relation  $k_{eff} \leq 1$  holds generally which means that the microscopic branching always causes the reduction of the effective crack driving force. This effect constitutes just a one part of the shielding effect. The second one is given by the fact that the length of a tortuous crack front is always higher than that of a straight one (of the same projective length). Hence, the work needed for creation of new surfaces is also higher when considering the same elementary advance of both cracks in the macroscopic direction.

Considering both the above mentioned shielding contributions, the global (averaged) effective stress intensity factor  $k_{effg}$  can be expressed as

$$k_{effg}^2 = \frac{\frac{1}{B} \int_0^B k_{eff}^2 dz}{R_L} = \frac{k^{*2}}{R_L} = \frac{g^*}{R_L}, \quad (2)$$

where  $B$  is the specimen thickness,  $z$  is the Cartesian coordinate along the thickness and  $R_L$  is the averaged linear roughness of the intergranular fracture surface [4]. Standardly measured value  $K_{Ic} = K_{Ic_e} + K_{Ic_i}$ , where the  $K_{Ic_i} = k_{effg} K_{Ic}$  is the intrinsic component and the  $K_{Ic_e}$  is the extrinsic one. The intrinsic component corresponds to the critical stress intensity value for the specimen of the same material containing a planar crack with a straight crack front of the

same projected length. This value is closely related to the inherent resistance of grain boundaries against the initiation of unstable crack growth, i.e. to the averaged grain boundary fracture energy. In order to obtain this value, the following steps are necessary:

1. construction of the real-like model of intergranular crack;
2. calculation of local values  $k_1, k_2, k_3$  along the crack front;
3. determination of the average linear roughness  $R_L$  of the intergranular fracture surface.

The first step can be realised by means of the computer procedure generating an intergranular crack within the 3D Voronoi tessellation simulating the grain boundary network [5,6]. The second problem can be solved using the program system FRANC3D [7] based on the boundary element method and requesting a computer with extended equipment. The third step demands the quantitative fractographical analysis of the real (or real-like) fracture surface.

The geometrical problem of a real-like intergranular crack can be transferred to a long planar crack ending by a narrow tortuous band as a part of the intergranular crack within the 3D Voronoi tessellation [8] – see Fig. 1. This case simulates well the stable growth of an elementary intergranular crack at the front of the transgranular fatigue precrack in a CT specimen during the fracture toughness test in corrosive environment or at a low temperature. Fig. 2 shows the variation of the local factor  $k_{eff}$  along the front of three real-like intergranular cracks of surface roughness in an extremely wide range  $R_L \in <1.1; 2.6>$  calculated by means of the FRANC3D program. It should be noted that most  $R_L$  values of hundreds generated intergranular cracks lie within the close range from 1.4 to 1.5 [6]. The  $k_{eff}$  and  $k_{effg}$  values for three real-like cracks of different  $R_L$  are shown in Tab. 1 obtained by numerical integration with respect to eq. (1) and (2). All values of normalised intrinsic fracture toughness  $k_{effg}$  are substantially lower than 1, i.e., the intrinsic fracture toughness is much more lower than the standardly measured  $K_{Ic}$  value. In other words, the roughness induced shielding level at intergranular crack fronts is very high since the average value  $k_{effg} = 0.61$  represents nearly 60 pct. increase in fracture toughness due to the pure geometrical effect of the crack microtortuosity.

Table 1. Values of effective stress intensity factors for real like intergranular crack fronts and for the related pyramidal model.

Model	Franc3D			pyramidal
	R11	R17	R26	
$R_L$	1.15	1.67	2.59	1.41
$k^*$	0.80	0.84	0.76	0.80
$k_{effg}$	0.75	0.65	0.47	0.67

The calculation of  $k_{effg}$  for real-like cracks represents a cumbersome and a very time consuming procedure. Therefore, a simple pyramidal model of the intergranular crack front, proposed in [3,9], is much more efficient for practical reasons. This model can be related to

the 3D Voronoi tessellation by using a regular 3D tessellation of the same mean grain size  $d_m$ . The oblique segments of the periodical pyramidal-like crack front are inclined by the angle  $\Phi = \pi/4$  to the virtual straight front lying in the macroscopic plane of the precrack. It corresponds to the value  $R_L = 1.41$  that agrees well with the average surface roughness values for intergranular cracks. The details of the model are described elsewhere [9].

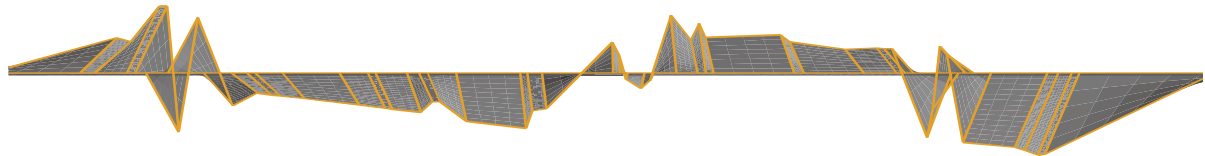


Fig. 1 Computer model of the intergranular crack front based on 3D Voronoi tessellation.

In Tab. 1, the value  $k_{effg} = 0.67$  is presented as determined for the pyramidal model related to all the three real-like crack fronts by the value  $d_m / \Delta a = 1.5$ , where  $\Delta a$  is the width of the pyramidal band. Physically it means that the plastic zone size at the moment of unstable fracture initiation becomes comparable to that of the mean grain. It yields optimal conditions for intergranular branching at the real crack front [10]. The value 0.67 agrees well with the average value 0.62 for the real-like cracks. This confirms the ability of the pyramidal model to approximate the averaged intergranular crack. The values  $k^*$  characterising only the contribution of the reduced crack driving force to the total shielding effect are also shown in Tab. 1. All  $k^*$  values are closely comparable. It means that the pyramidal model simulates well this shielding component for intergranular cracks regardless to the surface roughness.

### **CALCULATION OF THE ROUGHNESS INDUCED SHIELDING EFFECT IN UHSLA STEEL BY MEANS OF THE PYRAMIDAL MODEL**

Values of fracture toughness and impact absorbed energy of steels and cast irons are usually well correlated [11,12]. The pyramidal model can be applied to the elucidation of the inverse relation between fracture toughness and impact absorbed energy values found in the ultra-high strength low alloyed steel P-LDHA of the Czech provenience (AISI 4340 steel with increased Si content) [13]. Various heat treatments according to Tab. 2 resulted, in all cases, in the martensitic matrix type with different mean values of the prior austenite grain size. The standard heat treatment S1 – 870<sup>0</sup>C solution annealing and 300<sup>0</sup>C tempering – gives optimal tensile and fatigue mechanical properties whereas the 480<sup>0</sup>C tempering with the long delay corresponds to the degraded structure with a high concentration of carbide precipitates at prior austenite grain boundaries.

The yield strength of all specimens was nearly the same ( $\sigma_y = 1500$  MPa) as determined by the martensitic matrix.

Specimens of all variants of heat treatment were subjected to the standard fracture toughness test  $K_{Ic}$  using three-point bend specimen with fatigue precrack (FT specimens). Charpy V-notch and U-notch (2mm radius) impact toughness tests (CVN and UN specimens) were made as well. Results of mechanical tests are shown in Figs. 3 and 4. As can be clearly seen, the fracture toughness curve  $K_{Ic}$  vs.  $d$  is completely inverse to both the CVN- and UN absorbed energy.

Table 2. Heat treatment and mean prior austenite grain size

Solution annealing and quenching	Tempering	Symbol	Grain size [ $\mu\text{m}$ ]
870°C/1 h/oil	300°C/2h/air	S1	25
1050°C/1,5 h/oil	300°C/2h/air	S2	70
1200°C/1,5 h/oil	300°C/2h/air	S3	125
870°C/1 h/oil	480°C/5h/air	D1	25
1050°C/1,5 h/oil	480°C/5h/air	D2	70
1200°C/1,5 h/oil	480°C/5h/air	D3	125

Fracture morphology of S1 specimens was transgranular ductile with a very flat surface whereas both the S2 and S3 morphologies were predominantly intergranular (along prior austenite grain boundaries) with some transgranular cleavage facets. The coarse grained D2 and D3 specimens fractured intergranularly. However, shallow ductile dimples associated with carbide precipitates appeared at grain boundary facets. In the fine grained D1 specimen, the fatigue precrack was of intergranular microrelief unlike the rest of the fracture surface.

Fracture surface morphology near the notch differed substantially when comparing the fine grained and coarse grained UN or CVN samples. A wide shear zone adjacent to the notch surface is clearly distinguishable in case of the fine grained structure S1. On the other hand, the shear zones of coarse grained structures S3 and D3 are very narrow and much worse distinguishable.

Details of the fracture morphology of all the FT and UN samples are presented elsewhere [13].

The dependence  $k^*$  vs.  $d_m$  obtained by numerical integration within the framework of the pyramidal model ( $\Phi = \pi / 4$ ,  $\sigma_y = 1500 \text{ MPa}$ ) is shown in Fig. 5. The calculated values  $k_{effg}$  multiplied by the measured  $K_{Ic}$  value, i.e. the intrinsic  $K_{Ici}$  values, are plotted in Figs. 3 and 4. No shielding effect ( $k_{effg} = 1$ ) was assumed at the straight transgranular crack front in the S1 specimen.

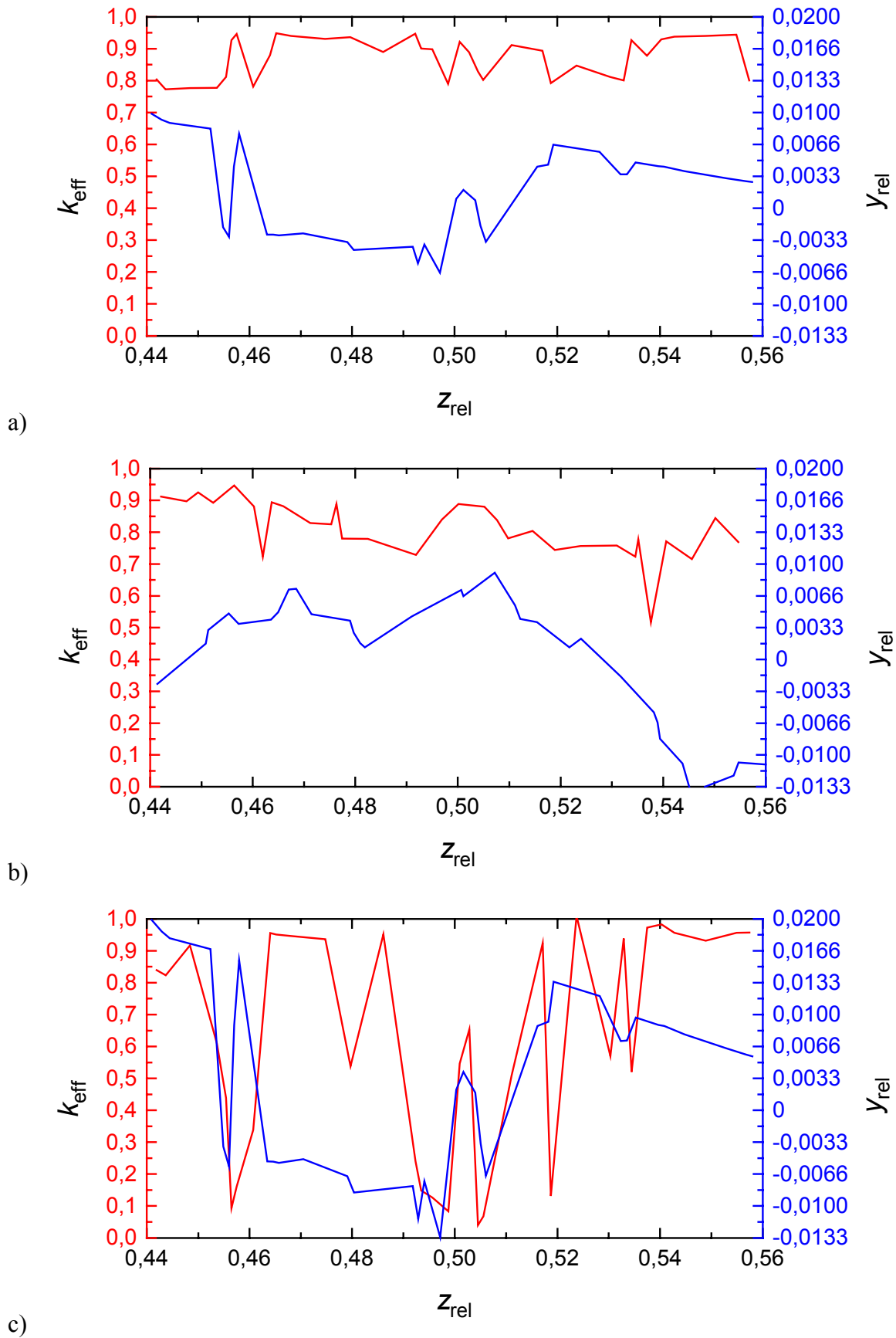


Fig. 2 Local effective stress intensity factors and crack shapes of real like intergranular crack fronts. a) model R11, b) model R17, c) model R26.

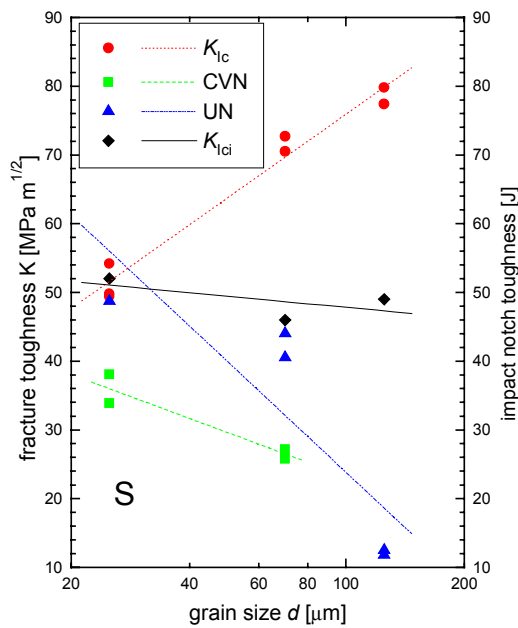


Fig. 3. Dependence of fracture- and notch toughness values on the mean austenite grain size for S-specimens.

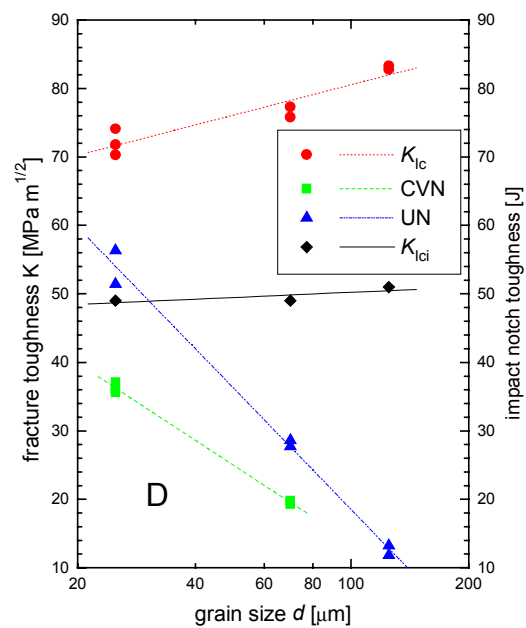


Fig. 4. Dependence of fracture- and notch toughness values on the mean austenite grain size for D-specimens.

The  $K_{Ici}$  values of all specimens are comparable and, as one would expect, those of intergranular S2 and S3 specimens are slightly lower than that of the transgranular S1 specimen. It shows again that the simple pyramidal crack front model yields a very satisfactory alternative to the real intergranular front. However, a partial splitting (forking) of the crack front can also accompany the intergranular fracture [1,14]. This phenomenon, which was not included into the calculation procedure, can additionally enhance the shielding level. Therefore, the real intrinsic values of all intergranularly fractured steel grades are, most probably, slightly shifted towards lower values than those of nearly  $50 \text{ MPa}\cdot\text{m}^{1/2}$ . In spite of this possible shift, the resistance of grain boundaries to the crack propagation seems to be not much lower than that of the grain interior. Since the D-grades were treated for the grain boundary embrittlement, one could rather expect the relation  $K_{Ici}(D) < K_{Ici}(S)$ . However, the shallow dimples at facets of D grades mean a more local plasticity at grain boundaries. This narrow ductile zone along grain boundaries was created due to the bounding of alloying elements in numerous grain boundary carbides [15]. It compensates the negative contribution of the pronounced grain boundary precipitation to the intrinsic fracture toughness.

In the CVN- and UN specimens, unlike in FT specimens, the crack must first nucleate within the plastic zone in the bulk and, after linking with the notch surface, it propagates further in an unstable manner. The linking mechanism operates mostly along planes with the highest resolved shear stress. In the initiation stage, both the high concentration of coarse carbides and the enhanced impurity level at grain boundaries produce a network of microcracks within the notch plastic zone of coarse grain structures. One of those intergranular crack nuclei

(sufficiently near to the free surface) initiates an easier linking process and subsequent unstable intergranular growth following the microcrack network. The shear zone near the notch is very narrow and the work needed for crack initiation is small. In fine grained structures, however, the crack initiates within the rather homogeneous plastic zone in the bulk in a relatively high distance from the free notch surface (site of a highest stress triaxiality). The linking process is accompanied by a large scale plastic strain because of a close free notch surface (plain stress state). Consequently, the shear zone is wide and the related crack initiation work is high. Since the crack initiation work creates a substantial part of the total absorbed energy, this value is smaller in intergranular fracture cases. From obvious reasons, both the density of grain boundary carbides and the size of dislocation pile-ups increase with increasing grain size. Hence, the crack initiation energy decreases in contradiction to the fracture toughness  $K_{Ic}$ .

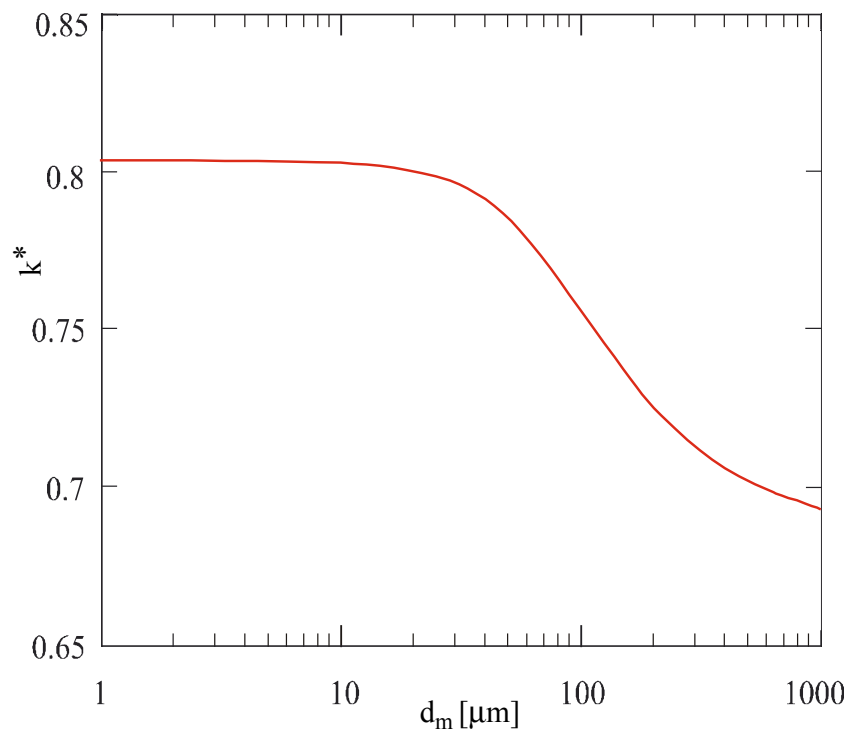


Fig. 5 Averaged normalised local stress intensity factor as function of mean grain size.

## CONCLUSION

The numerical calculation of the microroughness induced shielding level was performed for three real-like intergranular cracks with different surface roughness. The mean shielding level corresponds to the 60 pct. increase in the measured fracture toughness value against the inherent fracture toughness of grain boundaries. The simple pyramidal model approximating the complicated geometry of the real-like crack front yields values well comparable with the

averaged real-like data. This model was successfully used for quantitative elucidation of the inverse relation between the fracture and notch toughness found in ultra high strength low alloy steels.

## ACKNOWLEDGEMENT

This work was supported by the European agency COST (Action 517) and by the Ministry of Education and Youth of the Czech Republic under the Grant No. OC 517.30 (1998).

## REFERENCES

- [1] RITCHIE R.O.: Mat. Sci. Eng. A103, 1988, 15.
- [2] WANG J. and STEVENS R.: Mater. Science 24, 1989, 3421.
- [3] POKLUDA J., In: VII Summer School of Fracture Mechanics, Pokrzywna 2001, (in print).
- [4] POKLUDA J.: In: FRACTOGRAPHY 2000, ed. L. Parilák. Emilena Bratislava 2000, p. 82.
- [5] ŠANDERA P., PONÍŽIL P. and POKLUDA J.: In: FRACTOGRAPHY 97, ed. L. Parilák. ÚMS SAV Košice 1997, p. 151.
- [6] POKLUDA J., SAXL I., ŠANDERA P., PONÍŽIL P., MATOUŠEK M., PODRÁBSKÝ T. and HORNÍKOVÁ J.: In: Advances in Mechanical Behaviour, Plasticity and Damage - Euromat 2000, eds.: D.Miannay, P.Costa, D.Francois, A.Pineau. ELSEVIER 2000, p. 449
- [7] Ingrafea T. et al.: FRANC3D - 3D FRacture ANalysis Code. The Cornell University Fracture Group, Cornell University, Ithaca, NY 1996.
- [8] HORNÍKOVÁ J.: On the Linear Fracture Mechanics for Cracks with Microscopically Tortuous Front. PhD. Thesis. Brno UT 2000.
- [9] ŠANDERA P., POKLUDA J. and HORNÍKOVÁ J.: this proceedings.
- [10] POKLUDA, J. and SIEGL, J.: Fatigue Fract. Engng. Mater. Struct. 13, 1990, 375.
- [11] SERVER W. L.: In: ASM Handbook, Vol. 8, Mechanical Testing, J.R.Newby et al. eds., ASM International, 1992, p. 261.
- [12] KONEČNÁ R., HABASHI M. and SKOČOVSKÝ P.: Mémor. Etud. Scient. Rev. Métallurgie, 48, 1986, 149.
- [13] POKLUDA J., VLACH B., ŠANDERA P. and JURÁŠEK L.: In: Workshop of COST Action 517, ed. J.Lecomte-Beckers et al. Office for Official Publications of the European Communities, Luxembourg 2001, p. 126.
- [14] POKLUDA J.: In: Materials Science on the Onset of 3<sup>rd</sup> Millennium, ed. J. Švejcar. ÚMI FSI VUT a ČSNMT, Brno 1999, p. 104.
- [15] DOBROVSKÁ J., DOBROVSKÁ V., POKLUDA J., STRÁNSKÝ K., MANDRINO D. and JENKO M.: this proceedings.